International Journal of Control

Vol. 00, No. 00, Month 200x, 1–19

RESEARCH ARTICLE

Coverage control by multi-robot networks with limited-range anisotropic sensory

Katie Laventall[a] and Jorge Cortés[b*]

[a] *Department of Aeronautics and Astronautics, Stanford University, USA*

[b] *Department of Mechanical and Aerospace Engineering, University of California, San Diego, USA*

(*Received 00 Month 200x; final version received 00 Month 200x*)

This paper considers the deployment of a network of robotic agents with limited-range communication and anisotropic sensing capabilities. We encode the environment coverage provided by the network by means of an expected-value objective function. This function has a gradient which is not amenable to distributed computation. We provide a constant-factor approximation of this measure via an alternative aggregate objective function whose gradient is spatially distributed over the limited-range Delaunay proximity graph. We characterize the smoothness properties of the aggregate expected-value function and propose a distributed deployment algorithm that enables the network to optimize it. Simulations illustrate the results.

Keywords: Cooperative control; Distributed algorithms; Network deployment; Anisotropic, limited-range sensors; Locational optimization; Voronoi partitions

1 Introduction

Currently there is a large interest in the design of stable and decentralized control laws for distributed motion coordination. In this paper, we focus on the deployment of a robotic network where each agent is equipped with limited-range communication and sensing capabilities. The

*Corresponding author. Email: cortes@ucsd.edu

ISSN: 0020-7179 print/ISSN 1366-5820 online

DOI: 10.1080/0020717YYxxxxxxxx

http://www.informaworld.com

footprint of each sensor is a wedge-shaped region centered about each robot's orientation with an angular width less than or equal to π radians. We refer to these sensing capabilities as anisotropic. Our objective is to design distributed coordination algorithms that optimize sensor network coverage of a convex closed environment.

The literature on coordination tasks for robotic systems is becoming quite extensive. The deployment problem considered here falls within the field of facility location Okabe et al. (2000), Du et al. (1999), Drezner (1995), where one seeks to optimize the position of a collection of resources in order to provide better quality-of-service. In particular, this paper builds on Cortés et al. (2004), which provides an overview of coverage control for mobile networks, and Cortés et al. (2005), which models systems with limited-range, omnidirectional interactions. Other works on coverage problems include Howard et al. (2002), Hussein and Stipanovič (2007), Arsie and Frazzoli (2007), Kwok and Martínez (2007). To our knowledge, coverage optimization and control with limited-range, anisotropic sensory has not being studied in the literature. The sensor model considered in this paper leads to interactions among agents which are not omnidirectional but are rather defined along specific directions. The wedge-shaped sensor footprint poses nontrivial challenges on the distributed optimization of the network coverage. Our technical approach uses concepts and notions from computational geometry and geometric optimization, such as Voronoi partitions Okabe et al. (2000), proximity graphs Jaromczyk and Toussaint (1992), and spatially distributed maps Cortés et al. (2005).

The contributions of the paper are threefold. First, we define a novel proximity graph, termed the limited-range wedge graph. We show that a node can compute its neighbors in the limited-range wedge graph if it knows the position of its neighbors in the limited-range Delaunay graph. We refer to this property by saying that the limited-range wedge graph is distributed over the limited-range Delaunay graph. Second, we introduce the *expected-value* locational optimization function to measure the network coverage of the environment. Motivated by the fact that the gradient of this function is not amenable to distributed computation, we provide a constant-factor approximation via an alternative *aggregate expected-value* objective function. Both objective

functions incorporate the limited sensing capabilities of the network agents.

We characterize the smoothness properties of the aggregate expected-value function and show that the limited-range wedge graph plays a key role in the computation of its gradient. As an important consequence, we show that the gradient is spatially distributed over the limited-range Delaunay graph, i.e., we show that each agent can compute its corresponding component of the gradient only with information about the position of its neighbors in the limited-range Delaunay graph. Third, we propose a distributed gradient ascent algorithm to optimize network coverage, characterize its asymptotic convergence properties, and provide simulations to illustrate the algorithm execution.

The organization of this paper is as follows. Section 2 presents useful concepts on Voronoi partitions, proximity graphs, and spatially distributed maps. Section 3 introduces the expected-value and aggregate expected-value functions, discusses a constant-factor approximation between them, and analyzes their distributed character. Based on these results, Section 4 presents a deployment algorithm spatially distributed over the limited-range Delaunay graph and illustrates it in simulation. Section 5 gathers our conclusions and ideas for future work.

2 Preliminary developments

In this section we present various notational conventions and discuss notions from computational geometry. Let $\mathbb{R}$, $\mathbb{R}_{>0}$, and $\mathbb{R}_{\geq 0}$ be the set of real, positive real, and non-negative real numbers. Let $\mathbb{F}(\mathbb{R}^d)$ be the set of all finite pointsets in $\mathbb{R}^d$. For $x \in \mathbb{R}^d$, let $x^{\mathbf{T}}$ denote the transpose of x. Given a set S in $\mathbb{R}^d$, let $\mathrm{co}(S)$ and $\mathrm{int}(S)$ be the convex hull and the interior of S, respectively. The *indicator function* $1_S : \mathbb{R}^d \to \mathbb{R}$ of the set S is defined by $1_S(q) = 1$ if $q \in S$ and $1_S(q) = 0$ if $q \notin S$. For $\phi : \mathbb{R}^d \to \mathbb{R}_{\geq 0}$ integrable, let $\mathrm{area}_\phi(S) = \int_S \phi(x)dx$. Let $\overline{B}(x, r)$ denote the closed ball centered at x with radius r, and $\mathrm{arc}(x, r)$ denote an arc segment of $\partial\overline{B}(x, r)$. Throughout the paper, $Q \subset \mathbb{R}^2$ denotes a simple convex polygon. The *diameter* of Q is $\mathrm{diam}(Q) = \max_{q,p\in Q} \|q -$

$p\|$. Lastly, we define the unit vector $u_\theta = [\cos\theta, \sin\theta]^{\mathbf{T}}$ and the counterclockwise rotation matrix

$$\mathrm{Rot}_\theta = \begin{pmatrix} \cos\theta & -\sin\theta \\ \sin\theta & \cos\theta \end{pmatrix}.$$

2.1 *Voronoi partitions and boundary parametrizations*

Voronoi partitions can be defined in arbitrary metric spaces, but here we restrict our attention to the plane. The *Voronoi partition* generated by $\mathcal{P} = \{p_1, \ldots, p_n\} \subset \mathbb{R}^2$ is the collection $\mathcal{V}(\mathcal{P}) = (V_1(\mathcal{P}), \ldots, V_n(\mathcal{P}))$ where,

$$V_i(\mathcal{P}) = \{q \in \mathbb{R}^2 \mid \|q - p_i\| \leq \|q - p_j\|, \text{ for all } p_j \in \mathcal{P}\}.$$

Often, we use the notation V_i instead of $V_i(\mathcal{P})$. Two robots i and j are Voronoi neighbors if $V_i \cap V_j \neq \emptyset$. The section of the boundary of $V_i(\mathcal{P})$ that corresponds to the intersection with $V_j(\mathcal{P})$ is counterclockwise parametrized as

$$\gamma_{ij}(t) = \frac{p_i + p_j}{2} + t\,\mathrm{Rot}_{\frac{\pi}{2}}(p_j - p_i), \quad t \in [c_i, d_i], \tag{1}$$

for some $c_i, d_i \in \mathbb{R}$. The corresponding outward unit normal vector is $n_{ij} = \frac{p_j - p_i}{\|p_j - p_i\|}$, see Figure 1(b).

The Voronoi partition of an ordered set of possibly coincident points is not well-defined. To deal with this situation, we introduce the immersion $i_{\mathbb{F}} : (\mathbb{R}^2)^n \to \mathbb{F}(\mathbb{R}^2)$ that maps P to the pointset $\mathcal{P}$ containing the distinct points in P. The cardinality of $\mathcal{P}$ is determined by whether P is an element of

$$\mathcal{S}_{\text{coinc}} = \{(p_1, \ldots, p_n) \in (\mathbb{R}^d)^n \mid p_i = p_j \text{ for some } i \neq j \in \{1, \ldots, n\}\}. \tag{2}$$

For $P \in \mathcal{S}_{\text{coinc}}$, we consider the Voronoi partition generated by $\mathcal{P} = i_{\mathbb{F}}(P)$.

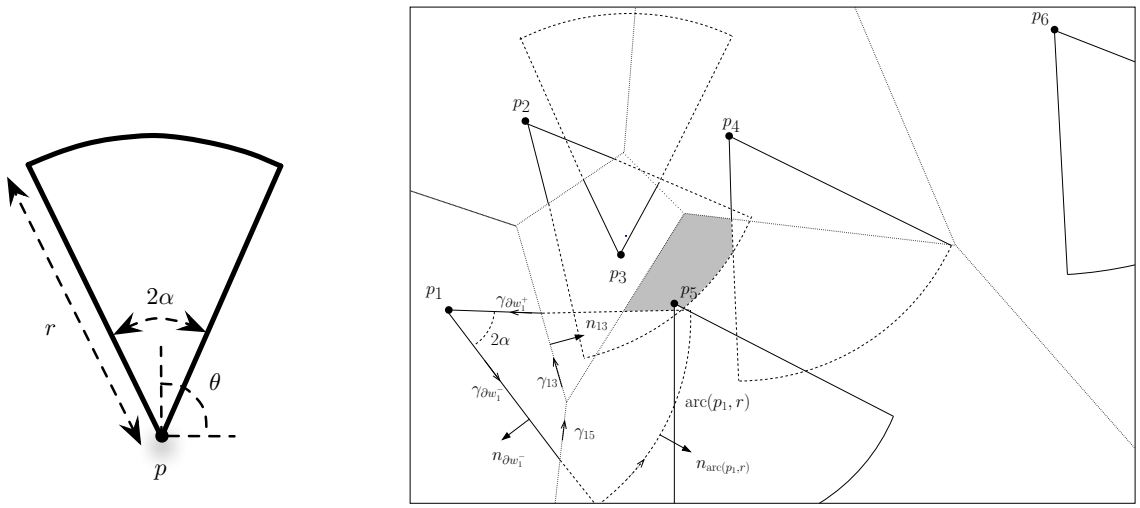

(a) (b)

Figure 1. (a) shows the wedge-shaped sensor footprint of an agent. (b) shows a random deployment of a robotic network, with the associated Voronoi partition. The notation for the various parametrizations of the Voronoi cell boundary and wedge sensing region are specified for p_1. The parameters for the wedge are $\alpha = \frac{\pi}{8}$ and $r = 0.5$. The shaded region in p_5's cell represents a subset of p_2's viewing wedge which cannot be computed by p_2 in a distributed way (see Section 3).

2.2 *Limited-range anisotropic sensory*

We model the robotic network so that each agent has limited-range anisotropic sensory. In other words, each agent has a sensor whose footprint is a circular sector with finite radius. More specifically, let $P = (p_1, \ldots, p_n) \in Q^n$ be a tuple of points in Q, where p_i is the position of robot i, and let $\Theta = (\theta_1, \ldots, \theta_n) \in (\mathbb{S}^1)^n$ be a tuple of angles, where θ_i is the orientation of robot i. For $P \in Q^n$ and $\Theta \in (\mathbb{S}^1)^n$, we denote $((p_1, \theta_1), \ldots, (p_n, \theta_n)) \in (\mathbb{R}^2 \times \mathbb{S}^1)^n$ by (P, Θ) with a slight abuse of notation. We define the wedge-shaped sensory region $w_{r,\alpha}(p, \theta)$ as the sector of a circle centered at p with radius r, orientation θ, and amplitude 2α, $\alpha \in (0, \frac{\pi}{2}]$, see Figure 1(a). For brevity, we occasionally denote the region $w_{r,\alpha}(p_i, \theta_i)$ of robot i by w_i. Alternatively, the region $w_{r,\alpha}(p, \theta)$ can be defined via its indicator function as

$$1_{w_{r,\alpha}(p,\theta)}(q) = \begin{cases} 1, & \text{if } \|q-p\| \le r \text{ and } \arccos\left(\frac{|(q-p)\cdot(\cos\theta, \sin\theta)|}{\|q-p\|}\right) \le \alpha, \\ 0, & \text{otherwise.} \end{cases}$$

It is convenient to decompose the boundary $\partial w_{r,\alpha}(p, \theta)$ of the wedge into the union of two line segments ∂w^+, ∂w^- and an arc segment $\text{arc}(p, r)$. We consider the following counterclockwise

parametrization of $\partial w_{r,\alpha}(p,\theta)$,

$$\gamma_{\partial w^-}(t) = p + t u_{\theta-\alpha}, \qquad t \in [0, r], \tag{3a}$$

$$\gamma_{\mathrm{arc}(p,r)}(t) = p + r u_{\theta+t}, \qquad t \in [-\alpha, \alpha], \tag{3b}$$

$$\gamma_{\partial w^+}(t) = p + (r-t) u_{\theta+\alpha}, \quad t \in [0, r]. \tag{3c}$$

The corresponding outward normal vectors are

$$n_{\partial w^-}(q) = \mathrm{Rot}_{\frac{-\pi}{2}}\, u_{\theta-\alpha}, \qquad q \in \partial w^-, \tag{4a}$$

$$n_{\mathrm{arc}(p,r)}(q) = \frac{q-p}{\|q-p\|}, \qquad q \in \mathrm{arc}(p,r), \tag{4b}$$

$$n_{\partial w^+}(q) = \mathrm{Rot}_{\frac{\pi}{2}}\, u_{\theta+\alpha}, \qquad q \in \partial w^+. \tag{4c}$$

These parametrizations are illustrated in Figure 1(b).

2.3 *Proximity graphs and spatially distributed maps*

The notion of proximity graph is useful to model the changing interactions in a mobile network, see Cortés et al. (2005), Jaromczyk and Toussaint (1992). A proximity graph function assigns to a pointset a graph whose vertex set is the pointset, and whose edge set is determined by the relative state of its vertices. Here we only consider proximity graphs defined for points in $X = \mathbb{R}^2$ or $X = \mathbb{R}^2 \times \mathbb{S}^1$. Let $\mathbb{G}(X)$ be the set of directed graphs whose vertex set is an element of $\mathbb{F}(X)$. A *proximity graph function* $\mathcal{G} : \mathbb{F}(X) \to \mathbb{G}(X)$ associates to $\mathcal{V} \in \mathbb{F}(X)$ a graph with vertex set $\mathcal{V}$ and edge set $\mathcal{E}_{\mathcal{G}}(\mathcal{V})$, where $\mathcal{E}_{\mathcal{G}} : \mathbb{F}(X) \to \mathbb{F}(X \times X)$ has the property that $\mathcal{E}_{\mathcal{G}}(\mathcal{V}) \subseteq \mathcal{V} \times \mathcal{V} \setminus \mathrm{diag}(\mathcal{V} \times \mathcal{V})$. The following proximity graph functions are relevant to our discussion:

(i) the *r-disk graph* $\mathcal{P} \mapsto \mathcal{G}_{\mathrm{disk}}(\mathcal{P}, r) = (\mathcal{P}, \mathcal{E}_{\mathcal{G}_{\mathrm{disk}}}(\mathcal{P}, r))$, with

$$\mathcal{E}_{\mathcal{G}_{\mathrm{disk}}}(\mathcal{P}, r) = \{(p_i, p_j) \in \mathcal{P} \times \mathcal{P} \setminus \mathrm{diag}(\mathcal{P} \times \mathcal{P}) \mid \|p_i - p_j\| \leq r\};$$

(ii) the *Delaunay graph* $\mathcal{P} \mapsto \mathcal{G}_D(\mathcal{P}) = (\mathcal{P}, \mathcal{E}_{\mathcal{G}_D}(\mathcal{P}))$, with

$$\mathcal{E}_{\mathcal{G}_{\mathrm{D}}}(\mathcal{P}) = \{p_i, p_j \in \mathcal{P} \times \mathcal{P} \setminus \mathrm{diag}(\mathcal{P} \times \mathcal{P}) \mid V_i \cap V_j \neq \emptyset\};$$

(iii) the *r-limited (or limited-range) Delaunay graph* $\mathcal{P} \mapsto \mathcal{G}_{\mathrm{LD}}(\mathcal{P}, r) = (\mathcal{P}, \mathcal{E}_{\mathcal{G}_{\mathrm{LD}}}(\mathcal{P}, r))$, with edges $(p_i, p_j) \in \mathcal{P} \times \mathcal{P} \setminus \mathrm{diag}(\mathcal{P} \times \mathcal{P})$ if

$$\big(V_i(\mathcal{P}) \cap \overline{B}(p_i, \tfrac{r}{2})\big) \cap \big(V_j(\mathcal{P}) \cap \overline{B}(p_j, \tfrac{r}{2})\big) \neq \emptyset\,;$$

(iv) the (r, α)*-limited (or limited-range) wedge graph* $(\mathcal{P}, \Theta) \mapsto \mathcal{G}_{\mathrm{LW}}(\mathcal{P}, \Theta) = (\mathcal{P}, \mathcal{E}_{\mathcal{G}_{\mathrm{LW}}}(\mathcal{P}, \Theta))$, with edges $((p_i, \theta_i), (p_j, \theta_j)) \in (\mathcal{P}, \Theta) \times (\mathcal{P}, \Theta)$ if

$$\big(V_i(\mathcal{P}) \cap V_j(\mathcal{P})\big) \cap w_{\frac{r}{2},\alpha}(p_i, \theta_i) \neq \emptyset.$$

Figure 2 presents an illustration of these notions. Note that the orientation of the robots does not affect the computation of the r-limited Delaunay graph. The r-limited Delaunay graph is undirected, whereas the (r, α)-limited wedge graph is directed. Clearly it is possible for $V_i \cap V_j \cap w_{r,\alpha}(p_i, \theta_i) \neq \emptyset$ and $V_i \cap V_j \cap w_{r,\alpha}(p_j, \theta_j) = \emptyset$ simultaneously, see for instance agents 1 and 3 in Figure 1(b).

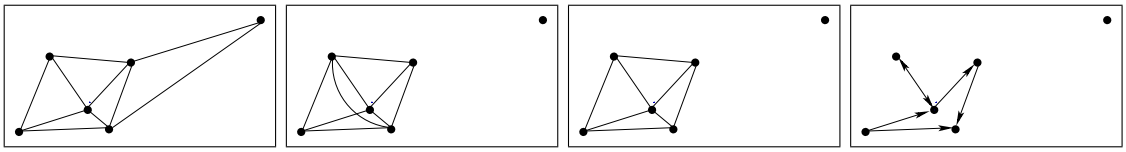

Figure 2. From left to right, Delaunay graph, r-disk graph, r-limited Delaunay graph, and (r, α)-limited wedge graph corresponding to the configuration in Figure 1(b).

To each proximity graph function $\mathcal{G}$, one can associate the *set of neighbors map* $\mathcal{N}_{\mathcal{G}} : \mathbb{F}(X) \to \mathbb{F}(X)$, defined by

$$\mathcal{N}_{\mathcal{G},v}(\mathcal{V}) = \{q \in \mathcal{V} \mid (v, q) \in \mathcal{E}_{\mathcal{G}}(\mathcal{V} \cup \{v\})\}.$$

For a directed proximity graph $\mathcal{G}$, q is an *in-neighbor* of v (or equivalently v is an *out-neighbor* of q) if $(q, v) \in \mathcal{E}_{\mathcal{G}}(\mathcal{V})$. To a vertex v, one can associate the set of *in-neighbors* and *out-neighbors*

maps $\mathcal{N}^{in}_{\mathcal{G},v}, \mathcal{N}^{\text{out}}_{\mathcal{G},v} : \mathbb{F}(X) \to \mathbb{F}(X)$ defined by

$$\mathcal{N}^{\text{in}}_{\mathcal{G},v}(\mathcal{V}) = \{q \in \mathcal{V} \mid (q, v) \in \mathcal{E}_{\mathcal{G}}(\mathcal{V} \cup \{v\})\},$$

$$\mathcal{N}^{\text{out}}_{\mathcal{G},v}(\mathcal{V}) = \{q \in \mathcal{V} \mid (v, q) \in \mathcal{E}_{\mathcal{G}}(\mathcal{V} \cup \{v\})\}.$$

Let $\mathcal{G}_1$ be a directed proximity graph and let $\mathcal{G}_2$ be an undirected proximity graph. Then, $\mathcal{G}_1$ is *spatially distributed* over $\mathcal{G}_2$ if, for all $\mathcal{V} \in \mathbb{F}(X)$ and all $v \in \mathcal{V}$, $\mathcal{N}^{\text{in}}_{\mathcal{G}_1,v}(\mathcal{V}) = \mathcal{N}^{\text{in}}_{\mathcal{G}_1,v}(\mathcal{N}_{\mathcal{G}_2,v}(\mathcal{V}))$ and $\mathcal{N}^{\text{out}}_{\mathcal{G}_1,v}(\mathcal{V}) = \mathcal{N}^{\text{out}}_{\mathcal{G}_1,v}(\mathcal{N}_{\mathcal{G}_2,v}(\mathcal{V}))$. Roughly speaking, this means that node v can compute its in- and out-neighbors in the graph $\mathcal{G}_1$ only with the information about the position of its neighbors in the graph $\mathcal{G}_2$. The following result establishes a useful property that will be instrumental later in characterizing the distributed character of the gradient of the locational optimization functions encoding the network coverage of the environment. For notational consistency, in the statement of the result, $\mathcal{G}_{\text{LD}}$ is considered to be defined on $X = \mathbb{R}^2 \times \mathbb{S}^1$ (where agent orientations do not play any role in determining the edge set).

Lemma 2.1: *The (r, α)-limited wedge graph $\mathcal{G}_{\text{LW}}$ is spatially distributed over the r-limited Delaunay graph $\mathcal{G}_{\text{LD}}$.*

Proof Note that $V_i(\mathcal{P}) \cap V_j(\mathcal{P}) \cap w_{\frac{r}{2},\alpha}(p_i, \theta_i) \neq \emptyset$ implies that $\overline{B}(p_i, \frac{r}{2}) \cap \{q \in \mathbb{R}^2 \mid \|q - p_i\| = \|q - p_j\|\} \neq \emptyset$. The latter is equivalent to $\overline{B}(p_j, \frac{r}{2}) \cap \{q \in \mathbb{R}^2 \mid \|q - p_i\| = \|q - p_j\|\} \neq \emptyset$. Therefore,

$$\begin{aligned}
\mathcal{N}^{\text{out}}_{\mathcal{G}_{\text{LW}},(p_i,\theta_i)}(\mathcal{P}, \Theta) &= \{(p_j, \theta_j) \in (\mathcal{P}, \Theta) \mid V_i(\mathcal{P}) \cap V_j(\mathcal{P}) \cap w_{\frac{r}{2},\alpha}(p_i, \theta_i) \neq \emptyset\} \\
&= \{(p_j, \theta_j) \in \mathcal{N}_{\mathcal{G}_{\text{LD}},(p_i,\theta_i)}(\mathcal{P}, \Theta) \mid V_i(\mathcal{P}) \cap V_j(\mathcal{P}) \cap w_{\frac{r}{2},\alpha}(p_i, \theta_i) \neq \emptyset\} \\
&= \mathcal{N}^{\text{out}}_{\mathcal{G}_{\text{LW}},(p_i,\theta_i)}(\mathcal{N}_{\mathcal{G}_{\text{LD}},(p_i,\theta_i)}(\mathcal{P}, \Theta)),
\end{aligned}$$

A similar proof can be given for $\mathcal{N}^{\text{in}}_{\mathcal{G}_{\text{LW}},(p_i,\theta_i)}(\mathcal{P}, \Theta)$. □

Functions which are spatially distributed over proximity graphs do not necessarily have to be defined as graph functions. More generally, given a set Y and proximity graph function $\mathcal{G}$, the map $T : X^n \to Y^n$ is *spatially distributed* over $\mathcal{G}$ if there exists maps $\tilde{T}_i : X \times \mathbb{F}(X) \to Y^n$, for

$i \in \{1, \ldots, n\}$ with the property that for all $(v_1, \ldots, v_n) \in X^n$,

$$T_i(v_1, \ldots, v_n) = \tilde{T}_i(v_i, \mathcal{N}_{\mathcal{G},i}(v_1, \ldots, v_n)),$$

where T_i denoted the i^{th} component of T. Thus, to compute the i^{th} component of a spatially distributed function, one needs only to know the state of the vertex v_i and the state of its neighbors on the graph $\mathcal{G}(\mathcal{V})$. This generalization allows for objects like vector fields and set-valued maps to be interpreted as spatially distributed over proximity graphs when defined in the appropriate context.

3 Encoding network performance via locational optimization

We begin by introducing measures of the sensor coverage of the environment by the robotic network.

3.1 *Expected-value locational optimization functions*

Let $\phi : Q \to \mathbb{R}_{\geq 0}$ be an integrable *density* function. This function can be thought of as a measure of the probability of some event taking place over Q. Due to noise and interference, the sensor performance of robot i degrades at point q in proportion to the distance $\|q - p_i\|$. Therefore, we introduce a continuously differentiable, strictly positive, non-increasing *performance* function $f : \mathbb{R}_{\geq 0} \to \mathbb{R}_{\geq 0}$ to measure this degradation: $f(\|q - p_i\|)$ provides a quantitative assessment of sensor quality of the ith robot at point $q \in Q$. The results presented in the foregoing discussion also hold for piecewise differentiable performance functions with finite jump discontinuities as in Cortés et al. (2005). For the sake of simplicity, we restrict our presentation here to differentiable performance functions.

Consider then the *expected-value* locational optimization function $\mathcal{H} : (Q \times \mathbb{S}^1)^n \to \mathbb{R}_{\geq 0}$,

$$\mathcal{H}(P, \Theta) = \int_Q \max_{i \in \{1,\ldots,n\}} \left\{ f(\|q - p_i\|) 1_{W_{r,\alpha}(p_i, \theta_i)}(q) \right\} \phi(q) dq. \tag{5}$$

This function provides an expected value of the sensor network performance. Hence, it is of

interest to find maximizers of $\mathcal{H}$. However, its gradient is in general not spatially distributed over the limited-range Delaunay or limited-range wedge graphs. Figure 1(b) illustrates this assertion. The portion shown in gray of p_2's sensing region is contained within p_5's Voronoi cell. Therefore, the location of p_5 affects how the value of $\mathcal{H}$ changes with respect to the position of p_2. However, since p_2 has no information about the location of p_5 (because p_5 is not its neighbor in either the limited-range wedge or limited-range Delaunay graphs), it cannot determine the rate of change of $\mathcal{H}$ with respect to its position.

The approach we take is to provide an alternative objective function. For $P \in Q^n$ and $q \in Q$, define $\operatorname{argmin}(P, q) = \{p \in \mathcal{P} \mid \|q-p\| = \min_{i\in\{1,\dots,n\}} \|q-p_i\|\}$. We define the *aggregate expected-value* locational optimization function

$$\mathcal{H}_{\text{agg}}(P,\Theta) = \int_Q \max_{i\in\{1,\dots,n\}} \{f(\|q-p_i\|)\}\, 1_{\bigcup_{p_j\in\operatorname{argmin}(P,q)} w_{r,\alpha}(p_j,\theta_j)}(q)\phi(q)dq \tag{6}$$

For $P \notin \mathcal{S}_{\text{coinc}}$, the function $\mathcal{H}_{\text{agg}}$ can be rewritten as

$$\mathcal{H}_{\text{agg}}(P,\Theta) = \sum_{i=1}^{n} \int_{V_i(P)} f(\|q-p_i\|) 1_{w_{r,\alpha}(p_i,\theta_i)}(q)\phi(q)dq. \tag{7}$$

The function $\mathcal{H}_{\text{agg}}$ sums the individual sensor performance of the robots within the intersection of their respective sensing wedge and Voronoi cell. Note that the function is discontinuous at coincident configurations. Let us show next that $\mathcal{H}_{\text{agg}}$ provides a good approximation of $\mathcal{H}$ on suitable regions of the configuration space $(Q \times \mathbb{S}^1)^n$.

Proposition 3.1: *Consider the expected-value and aggregate expected-value objective functions, $\mathcal{H}$ and $\mathcal{H}_{agg}$ respectively. Then, for all $(P,\Theta) \in (Q\times\mathbb{S}^1)^n$,*

$$\mathcal{H}_{agg}(P,\Theta) \le \mathcal{H}(P,\Theta) \le \mathcal{H}_{agg}(P,\Theta) + \|f\|_\infty \operatorname{area}_\phi(Q),$$

where $\|f\|_\infty = \max_{x\in[0,\operatorname{diam} Q]} |f(x)|$. Additionally, for $A \in (0, \operatorname{area}_\phi(Q)]$, define

$$\Sigma_A = \{(P,\Theta) \in (Q\times\mathbb{S}^1)^n \mid \sum_{j=1}^{m} \operatorname{area}_\phi(V_j(i_{\mathbb{F}}(P)) \cap (\bigcup_{\substack{i \ s.t. \\ p_i = z_j}} w_{r,\alpha}(p_i,\theta_i))) \ge A\},$$

where recall $i_{\mathbb{F}}(P) = \{z_1, \ldots, z_m\}$. *Then, for all* $(P, \Theta) \in \Sigma_A$,

$$\mathcal{H}_{agg}(P,\Theta) \leq \mathcal{H}(P,\Theta) \leq \Big(1 + \frac{\|f\|_\infty \operatorname{area}_\phi(Q)}{A\, f(\operatorname{diam}(Q))}\Big)\mathcal{H}_{agg}(P,\Theta).$$

Proof The lower bounds in both approximations follow directly from the function definition in (5) and (6). For $P \notin \mathcal{S}_{\text{coinc}}$, we reason as follows. Using the fact that Q can be expressed as the union of the Voronoi cells, we deduce

$$\begin{aligned}
&\mathcal{H}(P,\Theta) - \mathcal{H}_{\text{agg}}(P,\Theta) \\
&\quad \leq \sum_{i=1}^{n} \int_{V_i} f(\|q - p_i\|)\big(\max_{j\in\{1,\ldots,n\}} \{1_{w_{r,\alpha}(p_j,\theta_j)}(q)\} - 1_{w_{r,\alpha}(p_i,\theta_i)}(q)\big)\phi(q)dq \\
&\quad = \sum_{i=1}^{n} \int_{V_i} f(\|q - p_i\|)\big(1_{\cup_{j=1}^{n} w_{r,\alpha}(p_j,\theta_j)}(q) - 1_{w_{r,\alpha}(p_i,\theta_i)}(q)\big)\phi(q)dq.
\end{aligned}$$

The i^{th} summand in the expression vanishes on $w_{r,\alpha}(p_i, \theta_i)$. Therefore, we can obtain the upper bound in the additive approximation from the above expression as

$$\begin{aligned}
\mathcal{H}(P,\Theta) - \mathcal{H}_{\text{agg}}(P,\Theta) &\leq \sum_{i=1}^{n} \int_{V_i \cap Q \setminus w_{r,\alpha}(p_i,\theta_i)} f(\|q - p_i\|)\phi(q)dq \\
&\leq \|f\|_\infty \operatorname{area}_\phi(Q \setminus \cup_{i=1}^{n} w_{r,\alpha}(p_i,\theta_i)) \leq \|f\|_\infty \operatorname{area}_\phi(Q).
\end{aligned}$$

A similar set of inequalities can be derived for $P \in \mathcal{S}_{\text{coinc}}$. The upper bound in the constant-factor approximation follows from the above upper bound and the fact that $\mathcal{H}_{\text{agg}}(P,\Theta) \geq f(\operatorname{diam}(Q)) \sum_{j=1}^{m} \operatorname{area}_\phi(V_j(i_{\mathbb{F}}(P)) \cap (\bigcup_{\substack{i \text{ s.t.} \\ p_i = z_j}} w_{r,\alpha}(p_i,\theta_i))) \geq A\, f(\operatorname{diam}(Q))$ on Σ_A. □

From the proof of Proposition 3.1, one can see that the better the area coverage of Q provided by the regions $\{V_i \cap w_{r,\alpha}(p_i,\theta_i)\}_{i=1}^{n}$, the better the approximation of $\mathcal{H}$ provided by $\mathcal{H}_{\text{agg}}$ is. From (6), configurations with larger values of $\mathcal{H}_{\text{agg}}$ also induce good area coverage of Q. Therefore, the maximization of $\mathcal{H}_{\text{agg}}$ naturally leads to regions of good approximations of $\mathcal{H}$.

Remark 1 : For $P \in Q^n$ such that $\|z_i - z_j\| > 2r$, for all $z_i, z_j \in i_{\mathbb{F}}(P)$, the values of $\mathcal{H}$ and $\mathcal{H}_{\text{agg}}$ coincide, i.e., $\mathcal{H}(P,\Theta) = \mathcal{H}_{\text{agg}}(P,\Theta)$, for all $\Theta \in (\mathbb{S}^1)^n$. •

3.2 *Smoothness properties of the aggregate expected-value function*

We next explore the smoothness properties of the function $\mathcal{H}_{\text{agg}}$.

Theorem 3.2: *Given a density function ϕ and a performance function f, the function $\mathcal{H}_{agg}$ is piecewise continuously differentiable. On $\mathcal{S}_{coinc}$, $\mathcal{H}_{agg}$ is discontinuous. On $\text{int}(Q)^n \setminus \mathcal{S}_{coinc}$, it is continuously differentiable and, for each $i \in \{1, \dots, n\}$, its gradient is given by*

$$\frac{\partial \mathcal{H}_{agg}}{\partial p_i} = \int_{V_i \cap w_i} \frac{\partial}{\partial p_i} f(\|q - p_i\|)\phi(q)dq \tag{8a}$$
$$+ \int_{V_i \cap (\partial w_i^+ \cup \partial w_i^-)} f(\|q - p_i\|)\phi(q)n(q)dq + \int_{V_i \cap w_i \cap \partial \overline{B}(p_i, r)} f(\|q - p_i\|)\phi(q)n(q)dq$$
$$+ \sum_{\substack{j=1 \\ j \neq i}}^{n} \Big(\int_{V_i \cap V_j \cap w_i} f(\|q - p_i\|)\phi(q)\frac{q - p_i}{\|p_j - p_i\|}dq - \int_{V_i \cap V_j \cap w_j} f(\|q - p_j\|)\phi(q)\frac{q - p_i}{\|p_j - p_i\|}dq \Big),$$

where $n(q)$ denotes the unit outward normal vector at q, and

$$\frac{\partial \mathcal{H}_{agg}}{\partial \theta_i} = \sum_{s \in \{+,-\}} s \int_{V \cap \partial w_i^s} \|q - p_i\| f(\|q - p_i\|)\phi(q)dq. \tag{8b}$$

Proof For $P \in \text{int}(Q)^n \setminus \mathcal{S}_{\text{coinc}}$, consider the expression (7) of $\mathcal{H}_{\text{agg}}$. Note that $f(\|q - p_i\|)$ is continuously differentiable and for fixed (P, Θ), the maps $q \mapsto f(\|q - p_i\|)$ and $q \mapsto \frac{\partial}{\partial P} f(\|q - p_i\|)$ are both measurable and integrable on $V_i \cap w_{r,\alpha}(p_i, \theta_i)$. Also note that since both the Voronoi partition and the wedge are convex sets, their intersection is also convex. By (Cortés et al. 2005, Proposition A.1), $\mathcal{H}_{\text{agg}}$ is continuously differentiable on $(\text{int}(Q)^n \setminus \mathcal{S}_{\text{coinc}}) \times (\mathbb{S}^1)^n$ and, for each $i \in \{1, \dots, n\}$,

$$\frac{\partial \mathcal{H}_{\text{agg}}}{\partial p_i}(P, \Theta) = \frac{\partial}{\partial p_i} \sum_{k=1}^{n} \int_{V_k \cap w_k} f(\|q - p_k\|)\phi(q)dq \tag{9}$$
$$= \int_{V_i \cap w_i} \frac{\partial}{\partial p_i} f(\|q - p_k\|)\phi(q)dq + \sum_{k=1}^{n} \int_{\partial(V_k \cap w_k)} f(\|\gamma - p_k\|)\phi(\gamma)n^{\mathbf{T}}(\gamma)\frac{\partial \gamma}{\partial p_i}d\gamma.$$

Next, we simplify the second term in the equation. The boundary $\partial(V_k \cap w_{r,\alpha}(p_k, \theta_k))$ is composed of a finite number of line segments and arcs, all of which have been parametrized in Section 2.1. We first integrate over the wedge boundary $V_k \cap \partial(w_{r,\alpha}(p_k, \theta_k)) = V_k \cap (\partial w_k^+ \cup \partial w_k^-) \cup_{l=1}^{m} \text{arc}_l(p_k, r)$, see (3). This integral is nonzero only when $k = i$. Note that when there is a displacement in the

position of p_i, the motion of $w_{r,\alpha}(p_i,\theta_i)$ (when projected along the appropriate normal vector) is exactly the same as p_i i.e., $n_{(\cdot)}^{\mathbf{T}}\frac{\partial \gamma_{(\cdot)}}{\partial p_i} = n_{(\cdot)}$. Hence,

$$\int_{V_i\cap(\partial w_k^+\cup\partial w_k^-)\cup_{l=1}^m \mathrm{arc}(p_i,r))} f(\|q-p_i\|)\phi(q) n_{(\cdot)}^{\mathbf{T}}\frac{\partial \gamma_{(\cdot)}}{\partial p_i}d\gamma$$
$$= \int_{V_i\cap(\partial w_i^+\cup\partial w_i^-)} f(\|q-p_i\|)\phi(q) n_{\partial w_i^{(\cdot)}}dq + \sum_{l=1}^m \int_{\mathrm{arc}_l(p_i,r)} f(\|q-p_i\|)\phi(q) n_{\overline{B}(p_i,r)}dq.$$

The remaining boundary segments that must be considered define the regions $V_k \cap V_j \cap w_{r,\alpha}(p_k,\theta_k)$, for $j \in \{1,\ldots,n\}$. To parametrize these boundaries, consider the map given in (1). The derivative of this map with respect to p_i is non-zero only for the regions $V_i \cap V_j \cap w_{r,\alpha}(p_i,\theta_i)$ and $V_j \cap V_i \cap w_{r,\alpha}(p_j,\theta_j)$, i.e., when $p_j \in \mathcal{N}^{\mathrm{in}}_{\mathcal{G}_{\mathrm{LW}},(p_i,\theta_i)}(P,\Theta)$ or $p_j \in \mathcal{N}^{\mathrm{out}}_{\mathcal{G}_{\mathrm{LW}},(p_i,\theta_i)}(P,\Theta)$, respectively. For both regions, we use the counterclockwise parametrization γ_{ij}. When $p_j \in \mathcal{N}^{\mathrm{in}}_{\mathcal{G}_{\mathrm{LW}},(p_i,\theta_i)}(P,\Theta)$ we compute,

$$n_{ij}^{\mathbf{T}}\frac{\partial \gamma_{ij}}{\partial p_i} = \frac{1}{2}n_{ij}^{\mathbf{T}} + \frac{t}{\|p_j-p_i\|}\mathrm{Rot}_{\frac{\pi}{2}}(p_j-p_i)$$
$$= \frac{1}{2}n_{ij}^{\mathbf{T}} + \frac{1}{\|p_j-p_i\|}(\gamma_{ij} - \frac{p_i+p_j}{2}) = \frac{\gamma_{ij}-p_i}{\|p_j-p_i\|}.$$

For $p_j \in \mathcal{N}^{\mathrm{out}}_{\mathcal{G}_{\mathrm{LW}},(p_i,\theta_i)}(P,\Theta)$, a similar computation is made using the inward normal vector $n_{ji} = -n_{ij}$. We place these formulations back into (9) to obtain the complete form of (8a).

Next, let us compute the partial derivative of $\mathcal{H}_{\mathrm{agg}}$ with respect to θ_i by considering the parametrizations given in (3). Since the boundary $\partial(w_{r,\alpha}(p_i,\theta_i)) \cap V_i$ contains the only parametrization with a dependency on θ_i, we have

$$\frac{\partial \mathcal{H}_{\mathrm{agg}}}{\partial \theta_i}(P,\Theta) = \int_{\partial(w_{r,\alpha}(p_i,\theta_i))\cap V_i} f(\|\gamma-p_i\|)\phi(\gamma) n^{\mathbf{T}}(\gamma)\frac{\partial \gamma}{\partial \theta_i}d\gamma.$$

Notice that the normal vector $n_{\overline{B}(p_i,r)}$ is orthogonal to $\frac{\partial \gamma_{\mathrm{arc}(p_i,r)}}{\partial \theta_i}$. Hence, we only consider the line segments $\partial w_i^+ \cap V_i$ and $\partial w_i^- \cap V_i$. For $q \in \partial w_i^+$ we compute,

$$n_{\partial w_i^+}^{\mathbf{T}}\frac{\partial \gamma_{\partial w_i^+}}{\partial \theta_i} = \|\gamma_{\partial w_i^+} - p_i\|.$$

Hence,

$$\int_{\partial w_i^+ \cap V_i} f(\|\gamma_{\partial w_i^+} - p_i\|)\phi(\gamma_{\partial w_i^+}) n(\gamma_{\partial w_i^+})^{\mathbf{T}} \frac{\partial \gamma_{\partial w_i^+}}{\partial \theta_i} d\gamma_{\partial w_i^+} = \int_{\partial w_i^+ \cap V_i} \|q - p_i\| f(\|q - p_i\|)\phi(q) dq.$$

A similar calculation for the integral over $\partial w_i^- \cap V_i$ completes the proof. □

Remark 2 : Using extension by continuity, we redefine the domain where $\mathcal{H}_{\text{agg}}$ is continuously differentiable to include the boundary of Q. •

Note that, according to (8), the gradient of $\mathcal{H}_{\text{agg}}$ depends only on the position and orientation of p_i as well as those of its in- and out-neighbors in the (r, α)-limited wedge graph $\mathcal{G}_{\text{LW}}$. Therefore, the gradient of $\mathcal{H}_{\text{agg}}$ is spatially distributed over the undirected version of $\mathcal{G}_{\text{LW}}$. The following result is then an immediate consequence of Theorem 3.2 and Lemma 2.1.

Corollary 3.3: *On* $\text{int}(Q)^n \setminus \mathcal{S}_{coinc}$*, the gradient of* $\mathcal{H}_{agg}$ *is spatially distributed over* $\mathcal{G}_{LD}$*.*

4 A coordination algorithm to optimize network performance

Here we present an algorithm to maximize the locational optimization function $\mathcal{H}_{\text{agg}}$. We implement our control law in continuous time and analyze its convergence properties. Assume the robotic agents evolve according to

$$\dot{p}_i = u_i, \quad \dot{\theta}_i = v_i, \quad i \in \{1, \ldots, n\}.$$

We implement a gradient ascent of the locational optimization function $\mathcal{H}_{\text{agg}}$. In other words, for agents not co-located with any other agent, we set

$$u_i = \begin{cases} \frac{\partial \mathcal{H}_{\text{agg}}}{\partial p_i} & p_i \in \text{int}(Q), \\ \text{pr}_Q(\frac{\partial \mathcal{H}_{\text{agg}}}{\partial p_i}) & p_i \in \partial Q, \end{cases} \qquad v_i = \frac{\partial \mathcal{H}_{\text{agg}}}{\partial \theta_i}, \tag{10a}$$

where pr_Q is the orthogonal projection onto Q of the gradient vector given in Theorem 3.2. For agents co-located with other agents at the same point p and associated Voronoi cell V, we define $S_i \subset \{+, -\}$ by specifying $s \in S_i$ if ∂w_i^s is not contained in the wedge of another agent located

at p. Then, we set

$$u_i = 0, \qquad v_i = \sum_{s \in S_i} s \int_{V \cap \partial w_i^s} \|q - p_i\| f(\|q - p_i\|) \phi(q) dq. \tag{10b}$$

We assume that the Voronoi partition is updated in continuous time. The vector field is discontinuous, so we understand the solutions in the Krasovskii sense, see Krasovskiĭ (1963), Filippov (1988).

Theorem 4.1: *Given a density function ϕ and a performance function f, the control law on $(Q \times \mathbb{S}^1)^n$ defined by* (10) *has the following properties:*

(i) the law is spatially distributed over the limited-range Delaunay graph $\mathcal{G}_{LD}(\mathcal{P}, 2r)$ and;

(ii) for each initial configuration $(P_0, \Theta_0) \in (Q \times \mathbb{S}^1)^n$, the Krasovskii solution that exactly satisfies (10) *monotonically optimizes $\mathcal{H}_{agg}$ and asymptotically converges to the union of $\mathcal{S}_{coinc}$ and the set of critical points of $\mathcal{H}_{agg}$.*

Proof Statement (i) follows from Corollary 3.3. Regarding statement (ii), consider the compact domain $(Q \times \mathbb{S}^1)^n$. By the definition of (10), the domain is strongly invariant for the closed-loop system, i.e., any trajectory starting in $(Q \times \mathbb{S}^1)^n$ remains in the domain. Along any Krasovskii solution of the system that exactly satisfies (10), we have outside $\mathcal{S}_{\text{coinc}}$,

$$\frac{d}{dt} \mathcal{H}_{\text{agg}}(P(t), \Theta(t)) = \sum_{i=1}^{n} \big(\frac{\partial \mathcal{H}_{\text{agg}}}{\partial p_i} u_i + \frac{\partial \mathcal{H}_{\text{agg}}}{\partial \theta_i} v_i \big).$$

According to (10), $\frac{d}{dt} \mathcal{H}_{\text{agg}} \geq 0$, and is only zero if the solution is at a critical point of $\mathcal{H}_{\text{agg}}$ on the domain $(Q \times \mathbb{S}^1)^n$. Therefore, while the solution is outside $\mathcal{S}_{\text{coinc}}$, the function $\mathcal{H}_{\text{agg}}$ is monotonically optimized. If the solution does not reach $\mathcal{S}_{\text{coinc}}$, then the application of the LaSalle Invariance Principle with the function $-\mathcal{H}_{\text{agg}}$, see e.g., Khalil (2002), guarantees that it will reach the set of critical points of $\mathcal{H}_{\text{agg}}$. Otherwise, the solution reaches $\mathcal{S}_{\text{coinc}}$ and stays in it according to (10b). This concludes the proof. □

Remark 1: One can also consider a similar control law for robotic agents with second-order dynamics of the form $\ddot{p}_i = u_i$, $\ddot{\theta}_i = v_i$, $i \in \{1, \ldots, n\}$. For instance, while on $\text{int}(Q)$, one can

adapt the control law (10a) as

$$u_i = \frac{\partial \mathcal{H}_{\text{agg}}}{\partial p_i} - k_1 \dot{p}_i, \qquad v_i = \frac{\partial \mathcal{H}_{\text{agg}}}{\partial \theta_i} - k_2 \dot{\theta}_i, \tag{11}$$

where $k_1, k_2 > 0$. For agents co-located with other agents, one can adapt (10b) similarly. The convergence of network trajectories that remain in $(Q \times \mathbb{S}^1)^n$ can be established as in Theorem 4.1 via the Lyapunov function $-\mathcal{H}_{\text{agg}} + \sum_{i=1}^n (\|\dot{p}_i\|^2 + \dot{\theta}_i^2)$. However, in general, the set $(Q \times \mathbb{S}^1)^n$ is not strongly invariant under (11). •

4.1 *Simulations*

To illustrate the performance of the network under the coordination algorithm (10), we present some numerical simulations. The algorithm is implemented in Mathematica® as a main program running the simulation that makes use of a library of routines. The structure of this simulation is loosely described by the following procedure: first, the intersection of the bounded Voronoi cell V_i and the wedge $w_{r,\alpha}(p_i, \theta_i)$, for $i \in \{1, \ldots, n\}$, is computed. Next, the r-limited Delaunay and (r, α)-limited wedge proximity graphs are constructed. Then, for each robot, information of its in- and out- neighbors is collected and used to construct the various parametrizations necessary for the gradient computation. Finally, the various surface and boundary integrals involved in the gradient of the locational optimization function $\mathcal{H}_{\text{agg}}$ are computed using the Mathematica® numerical integration routine `NIntegrate`. The position and orientation of each robot are then updated according to these results. Figure 3 illustrates an execution.

Figure 4 shows the evolution of the locational optimization functions $\mathcal{H}$ and $\mathcal{H}_{\text{agg}}$ for two different executions of (10) with $r = .35$ and $r = .5$. As forecasted by our analysis, $\mathcal{H}_{\text{agg}}$ is monotonically optimized. The fact that the evolution of $\mathcal{H}$ is monotonic too is in general not guaranteed. With the appropriate network configuration, the area coverage of Q provided by the regions $\{V_i \cap w_{r,\alpha}(p_i, \theta_i)\}_{i=1}^n$ improves as the value of r increases. According to the proof of Proposition 3.1, this implies that the approximation of $\mathcal{H}$ provided by $\mathcal{H}_{\text{agg}}$ improves. This fact can be observed comparing the differences between the final values of the objective functions in

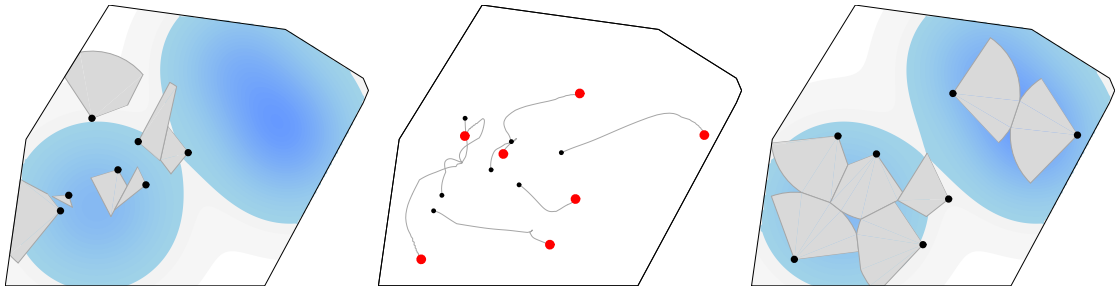

(a) (b) (c)

Figure 3. Execution of the coordination algorithm (10) by 7 robots with sensory wedge radius $r = 0.35$ and $\alpha = \frac{\pi}{4}$. The plot in (a) (resp. in (c)) illustrates the initial (resp. final) configuration after 5.5 centiseconds. The plot in (b) illustrates the gradient ascent flow of the system, with the smaller dots representing the initial configuration and the larger dots representing the final one. The performance function is $f(x) = 2 - x^2$ and the density function ϕ (represented by its contour plot) is the sum of three Gaussian functions of the form $50\, e^{-10((x-x_{\text{cntr}})^2+(y-y_{\text{cntr}})^2)}$.

Figure 4(a) and (b).

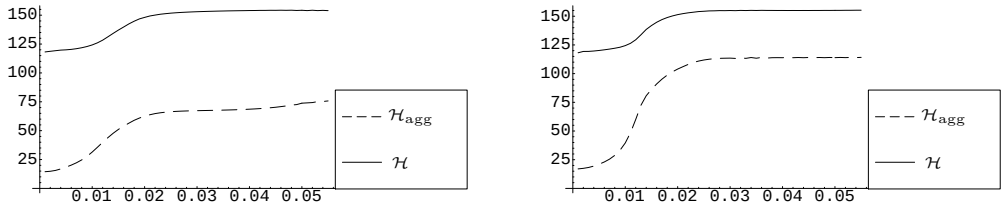

(a) (b)

Figure 4. Evolution of the locational optimization functions $\mathcal{H}$ (solid) and $\mathcal{H}_{\text{agg}}$ (dashed) along the execution of (10) with (a) $r = 0.35$ and (b) $r = 0.5$. The approximation of $\mathcal{H}$ provided by $\mathcal{H}_{\text{agg}}$ improves as the area coverage of Q provided by the regions $\{V_i \cap w_{r,\alpha}(p_i, \theta_i)\}_{i=1}^n$ improves.

5 Conclusions

We have introduced two locational optimization functions to measure the coverage of the environment provided by a group of robotic agents with limited-range anisotropic sensory. Based on considerations about the distributed computation of the gradient information, we have selected the aggregate expected-value function as our optimization criteria. We have characterized the smoothness properties of this objective function, computed its gradient, and characterized its spatially-distributed character. We have designed a continuous-time gradient ascent strategy that is guaranteed to achieve optimal network deployment. Further research will include

the characterization of the critical points of the objective function, the design and analysis of discrete-time coordination algorithms, the consideration of general agent dynamics, the synthesis of cooperative strategies to attain global optima of the aggregate objective function, and the study of similar deployment problems in nonconvex environments.

Acknowledgments

This research was partially supported by NSF CAREER award ECS-0546871.

References

Okabe, A., Boots, B., Sugihara, K., and Chiu, S.N., *Spatial Tessellations: Concepts and Applications of Voronoi Diagrams*, 2 ed., Wiley Series in Probability and Statistics, New York: John Wiley (2000).

Du, Q., Faber, V., and Gunzburger, M. (1999), "Centroidal Voronoi tessellations: Applications and algorithms," *SIAM Review*, 41(4), 637–676.

Drezner, Z. (ed.) *Facility Location: A Survey of Applications and Methods*, Springer Series in Operations Research, New York: Springer Verlag (1995).

Cortés, J., Martínez, S., Karatas, T., and Bullo, F. (2004), "Coverage Control for Mobile Sensing Networks," *IEEE Transactions on Robotics and Automation*, 20(2), 243–255.

Cortés, J., Martínez, S., and Bullo, F. (2005), "Spatially-Distributed Coverage Optimization and Control with Limited-Range Interactions," *ESAIM. Control, Optimisation & Calculus of Variations*, 11, 691–719.

Howard, A., Matarić, M.J., and Sukhatme, G.S. (2002), "Mobile Sensor Network Deployment using Potential Fields: A Distributed Scalable Solution to the Area Coverage Problem," in *International Conference on Distributed Autonomous Robotic Systems (DARS02)*, Jun., Fukuoka, Japan, pp. 299–308.

Hussein, I.I., and Stipanovič, D.M. (2007), "Effective coverage control for mobile sensor networks

with guaranteed collision avoidance," *IEEE Transactions on Control Systems Technology*, 15(4), 642–657.

Arsie, A., and Frazzoli, E. (2007), "Efficient routing of multiple vehicles with no communications," *International Journal on Robust and Nonlinear Control*, 18(2), 154–164.

Kwok, A., and Martínez, S. (2007), "Energy-balancing cooperative strategies for sensor deployment," in *IEEE Conf. on Decision and Control*, New Orleans, LA, pp. 6136–6141.

Jaromczyk, J.W., and Toussaint, G.T. (1992), "Relative neighborhood graphs and their relatives," *Proceedings of the IEEE*, 80(9), 1502–1517.

Krasovskiĭ, N.N., *Stability of motion. Applications of Lyapunov's second method to differential systems and equations with delay.*, Translated by J. L. Brenner, Stanford University Press (1963).

Filippov, A.F., *Differential Equations with Discontinuous Righthand Sides*, Vol. 18 of *Mathematics and Its Applications*, Dordrecht, The Netherlands: Kluwer Academic Publishers (1988).

Khalil, H.K., *Nonlinear Systems*, 3 ed., Englewood Cliffs, NJ: Prentice Hall (2002).